Available online at www.sciencedirect.com
ScienceDirect
Trans. Nonferrous Met. Soc. China 23(2013) 294−300
Transactions of Nonferrous Metals Society of China
www.tnmsc.cn

Production of Al−B master alloys by mixing KBF_4 salt into molten aluminum

Qing-liang WANG[1], Hong-sheng ZHAO[2], Zheng-guang LI[2], Li SHEN[2], Jiu-zhou ZHAO[1]

1. Institute of Metal Research, Chinese Academy of Sciences, Shenyang 110016, China;
2. Center for Quality Technology, Baotou Aluminum Co., Ltd., Baotou 014046, China

Received 15 December 2011; accepted 12 April 2012

Abstract: Two mixing techniques, the immersion method and the vortex method, were adopted in the production of Al−3%B master alloys since the generally used production route involving the direct addition of KBF_4 salt to molten aluminum has several drawbacks. The experimental results demonstrate that the Al−B master alloys produced by the immersion method show a microstructure characterized by the appearances of AlB_{12} phase and many agglomerations of boride particles, while the Al−B master alloy produced by the vortex method exhibits a well dispersed microstructure of AlB_2 particles in the matrix. The distinct microstructure features result from the differences in the stirring speed during the salt additions and the average size of the salt droplets achieved by the salt additions.

Key words: Al−B master alloy; agglomeration; AlB_{12}; mixing technique

1 Introduction

Al−B master alloys are widely used in the production of aluminum conductor to remove the transition metal impurities, such as titanium, vanadium, chromium and zirconium, which reduce the electrical conductivity of aluminum dramatically even at trace levels [1−3]. Al−B master alloys can also be used for the in situ fabrication of aluminum matrix composites. One example is the in situ fabrication of the AlB_2 fiber reinforced composites using the Al−5%B master alloy [4]. Besides, Al−B master alloys can be used as grain refiners for some aluminum alloys. Compared with the commonly used Al−Ti−B master alloys, they show a much higher grain refining efficiency for Al−Si alloys [5−7] and electrolytic low-titanium aluminum (ELTA) [8,9].

Several methods have been reported for the manufacturing of Al−B master alloys, including reaction of fluoride salt (KBF_4) with aluminum [5,10−13], melting of elemental blends [14,15], reaction of boron oxide (B_2O_3) with aluminum [16−18], powder metallurgy [19], mechanical alloying [20] and electrolysis [21]. Among them, for the sake of economy and practicality, the method involving the reaction of KBF_4 with molten aluminum is widely used in industry. Boron is reduced from fluoride salt by aluminum and disperses into aluminum melt in the form of aluminum borides, AlB_2 and AlB_{12}. Despite the wide range of applications, the production of Al−B master alloys has received very limited attention. Generally, the production of Al−B master alloys involves the direct addition of KBF_4 salt to molten aluminum [10]. It has been found that there are several drawbacks associated with this production route, such as the low boron recovery [5,20], the presence of AlB_{12} phase [5,10,11] and agglomeration of boride particles in master alloy [11]. The low boron recovery raises the cost of production and the other two drawbacks have a detrimental influence on the performance of Al−B master alloys [3,5,13].

Mixing techniques have been widely employed in industrial production processes. For example, in modern pyrometallurgical processes, the overall reaction rate is generally accelerated by mixing phases through gas injection [22]. In the fabrication of particulate metal matrix composites (PMMCs), a uniform distribution of the reinforcing particles in the matrix can be achieved by employing proper mixing techniques, such as the vortex method, gas injection of particles and zero gravity processing [23].

Two mixing techniques, the immersion method and

Foundation item: Project (u0837601) supported by the National Natural Science Foundation of China
Corresponding author: Qing-liang WANG; Tel/Fax: +86-24-23971905; E-mail: qlwang@imr.ac.cn
DOI: 10.1016/S1003-6326(13)62460-7

the vortex method, were adopted in the production of Al−B master alloys in an effort to avoid the presence of AlB_{12} phase and agglomeration of boride particle in the alloy product. The effect of the mixing condition on the microstructure formation in the master alloys was discussed in details.

2 Experimental

Commercial purity aluminum (99.7%) ingots and high purity KBF_4 (>99.0%) powders of 200−400 μm in diameter were used as raw materials. The production campaigns were carried out on a 1.2 kg batch scale. The intended nominal composition of master alloy was Al−3%B. Experiments were done by using a medium-frequency induction furnace (2000 Hz).

The salt mixing was carried out when aluminum was melted in a graphite crucible and overheated to 800 °C. In the immersion method, fluoride salt was first wrapped into five packets with aluminum foil. The packets were then immersed into aluminum melt with a graphite plunger one by one. After each immersion the melt was either manually stirred with a graphite rod or mechanically stirred with rotation speed of the graphite impeller of about 700 r/min (alloys 1 and 2 in Table 1). In the vortex method, as shown in Fig. 1, a vortex was first created by adjusting the rotation speed of the graphite impeller with inclined grooves on its surface to 600−700 r/min. KBF_4 powders were then added into the center of the vortex at a constant rate through a salt addition setup. KBF_4 powders were sucked into aluminum melt and reacted with aluminum (alloy 3). The duration of salt mixing lasted about 20 min.

Table 1 Mixing conditions employed in production of three master alloys and boron recovery

Alloy No.	Mixing technique	Stirring during mixing	Recovery rate of B/%
1	Immersion method	Manual	84.6
2	Immersion method	Mechanical	78.2
3	Vortex method	Mechanical	82.4

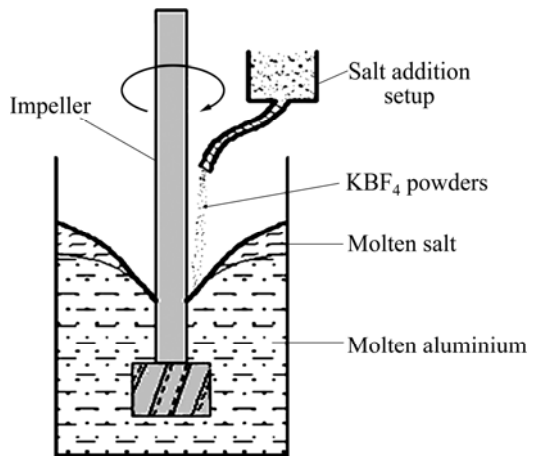

Fig. 1 Schematic illustration of experimental setup for mixing KBF_4 salt into molten aluminum using vortex method

After the graphite rod or impeller was pulled out from melt, the alloy melts were held at 800 °C for 30 min. At last, molten salt was decanted, and aluminum melt was stirred thoroughly with a graphite rod and poured into an iron mould.

The obtained ingots were sectioned through the centre line. Specimens for chemical analysis were cut at the center of the ingots. Samples were prepared following the standard metallographic procedures. Microstructure analysis of these samples was carried out by optical microscopy and phase identification was done by energy dispersive X-ray spectroscopy (EDS) and X-ray diffraction (XRD).

3 Results

The recovery rates of B of the master alloys produced under different mixing conditions are shown in Table 1. During the production of the Al−3%B master alloys, the amount of KBF_4 equivalent to 3.6%B was added assuming a loss of 20%. The B contents of the produced master alloys are all about 3%. Recovery rate of B (η) is calculated as follows:

$$\eta = \frac{m_1}{m_2} \times 100\% \quad (1)$$

where m_1 is B content in the master alloy; m_2 is the B content in KBF_4 added to produce the master alloy.

To our knowledge, the recovery rate of B is generally lower than 80% for the alloys produced by adding KBF_4 salt directly to molten aluminum [5,20]. The recovery rates of B of alloys 1 and 3 are both higher than 82%, as shown in Table 1. The relatively high recovery rate of B can be accounted for by the prohibition of the BF_3 gas emission when KBF_4 salt reacts with molten aluminum inside liquid metal. However, a lower recovery rate of 78.2% was obtained for alloy 2, which was produced by the immersion method followed by mechanical stirring after each immersion. This suggests that the vigorous stirring carried out after each immersion has an effect of weakening the prohibition of the BF_3 gas emission in the immersion method.

For alloy 1, the boride particles are severely segregated and some sizable agglomerations of boride particles are observed in the microstructure. Two typical ones are shown in Fig. 2. Figure 3 shows the EDS spectra of the phases existing in alloy 1. As shown in Figs. 3(a) and 3(b), the mole ratios of B to Al are about

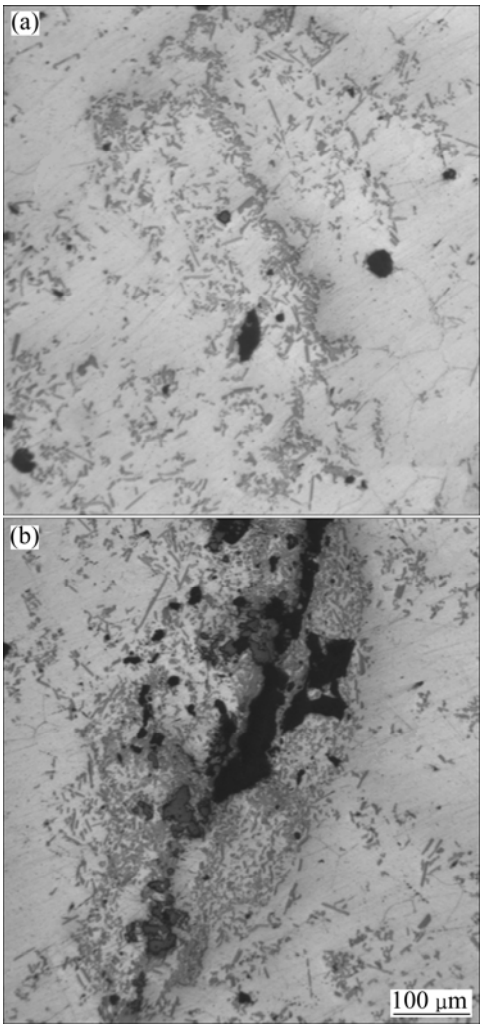

Fig. 2 Optical micrographs of two typical large agglomerations of boride particles in alloy 1 produced by immersion method followed by slow manual stirring after each immersion: (a) Chain-like agglomeration; (b) Agglomeration enveloping some black phases

7:3 and 15:1 for the light gray phase and the dark gray phase, respectively. According to the Al−B phase diagram [24], there exist only two kinds of stable aluminum borides, AlB_2 and AlB_{12}, in molten aluminum. As boron is a light element, the accuracy of the analyzing results with EDS is not high. It is thus concluded that the light gray phase is AlB_2 and the dark gray phase is AlB_{12}. Figure 3(c) shows that the black phase consists of F, Al and K and the mole ratio of F to Al to K is about 4:1:1. Thus the slag inclusion is mainly comprised of $KAlF_4$.

The chain-like agglomerations, as shown in Fig. 2(a), consist of only AlB_2 phase. This kind of agglomeration is also found in the master alloys prepared by adding KBF_4 salt directly to the aluminum melt [11]. They are probably formed at the interface between molten aluminum and the floating molten salt. The other typical ones are characterized by the aggregated boride

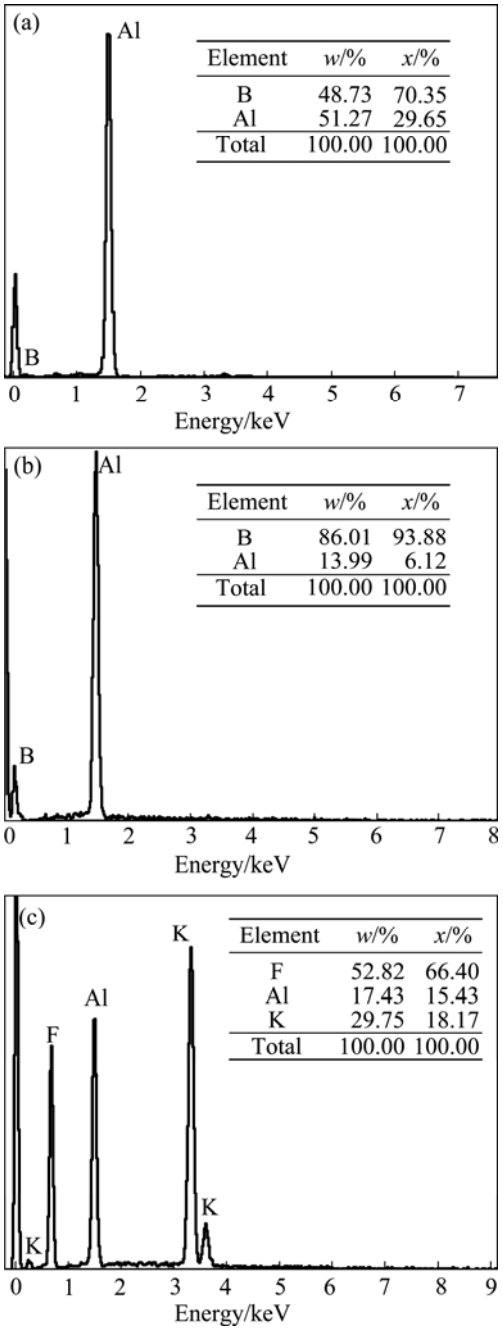

Fig. 3 EDS spectra of light gray phase (a), dark gray phase (b) and black phase (c) in alloy 1

particles of both AlB_2 and AlB_{12} surrounding some residual salt (Fig. 2(b)). This type of agglomerations has not been reported in the literature. They are formed at the interface between molten aluminum and salt droplets during adding KBF_4 into molten aluminum by the vortex method.

The microstructure of alloy 2 is shown in Fig. 4. No large agglomerations are found in the microstructure and the boride particles are distributed in the aluminum matrix mainly in the form of small agglomerations. This can be attributed to the breaking up effects of the vigorous stirring to the large boride agglomerations. It is

consistent with the results of JACKSON et al [13] which demonstrated that mechanical stirring could efficiently break up the large boride agglomerations, and result in a uniform distribution of small-sized agglomerations in the matrix. AlB_{12} phase is also found in the alloy.

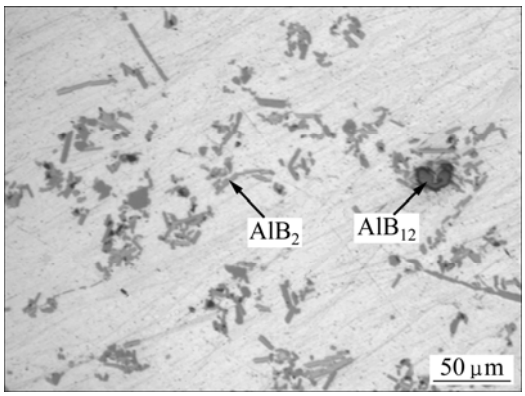

Fig. 4 Microstructure of alloy 2 produced by immersion method followed by mechanical stirring after each immersion

The microstructure and XRD pattern of alloy 3 are shown in Fig. 5 and Fig. 6, respectively. It can be seen that there is no AlB_{12} phase in the alloy and the AlB_2 particles are well dispersed in the matrix mainly in the form of individual particles.

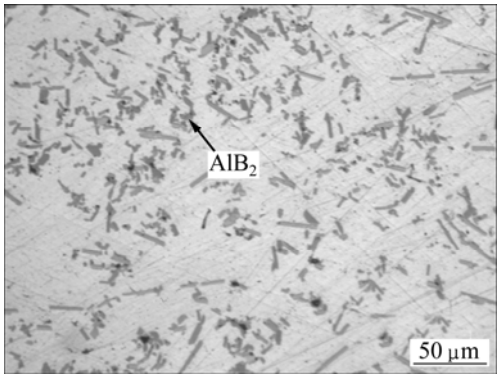

Fig. 5 Microstructure of alloy 3 produced by vortex method

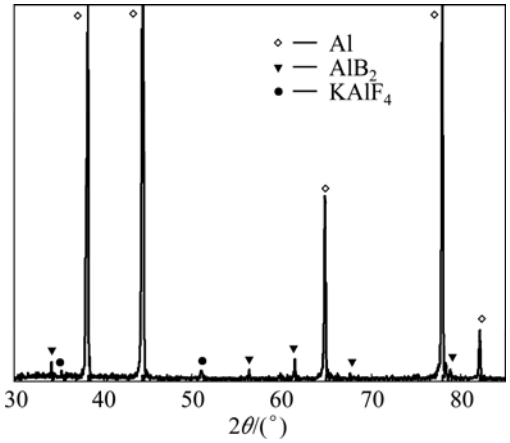

Fig. 6 XRD pattern of alloy 3 produced by vortex method

4 Discussion

KBF_4 salt melted quickly after being mixed into molten aluminum. Some of the molten salt would float up to the surface of molten aluminum due to the gravity effect, while most would disperse in the aluminum melt in the form of salt droplets.

The decomposition of KBF_4 droplets is [25]

$$KBF_4(l)=KF(l)+BF_3(g) \quad (2)$$

The BF_3 gas emission is prohibited by the surrounding liquid metal and a reduction of the fluoride gas takes place at the droplet-aluminum interface.

$$BF_3(g)+[Al]=[B]+AlF_3(l) \quad (3)$$

The produced AlF_3 transfers into the salt droplet and reacts with KF produced in reaction (2).

$$AlF_3(l)+KF(l)=KAlF_4(l) \quad (4)$$

The remaining KBF_4 salt in the salt droplet is also reduced by the aluminum melt.

$$KBF_4(l)+[Al]=[B]+KAlF_4(l) \quad (5)$$

The released boron atoms in reactions (3) and (5) are diffused into the liquid aluminum, resulting in the enrichment of boron at the droplet-aluminum interface. Boride particles would be precipitated at the interface with the increase of boron concentration:

$$Al(l)+2[B]=AlB_2(s) \quad (6)$$

$$Al(l)+12[B]=AlB_{12}(s) \quad (7)$$

The free energy change of reaction (6) for the formation of 1 mol AlB_2 and the free energy change of reaction (7) for the formation of 1 mol AlB_{12} can be given by

$$\Delta G_{(6)}=\Delta G_{(6)}^{\Theta}-RT\ln[(C_{[B]})^2C_{[Al]}] \quad (8)$$

$$\Delta G_{(7)}=\Delta G_{(7)}^{\Theta}-RT\ln[(C_{[B]})^{12}C_{[Al]}] \quad (9)$$

where R is the gas constant; T is the thermodynamic temperature; $C_{[B]}$ and $C_{[Al]}=1-C_{[B]}$ are the mole fractions of boron and aluminum in the aluminum melt at the droplet−aluminum interface, respectively; $\Delta G_{(6)}^{\Theta}$ and $\Delta G_{(7)}^{\Theta}$ are the standard free energy changes of reactions (6) and (7), respectively, which can be calculated as [24]

$$\Delta G_{(6)}^{\Theta}=G_{AlB_2}^{\Theta}-G_{Al}^{\Theta Liq}-2G_B^{\Theta Liq} \quad (10)$$

$$\Delta G_{(7)}^{\Theta}=G_{AlB_{12}}^{\Theta}-G_{Al}^{\Theta Liq}-12G_B^{\Theta Liq} \quad (11)$$

$$G_{AlB_2}^{\Theta}=G_{Al}^{\Theta S}+2G_B^{\Theta S}-23000-3.05T \quad (12)$$

$$G_{AlB_{12}}^{\Theta}=G_{Al}^{\Theta S}+12G_B^{\Theta S}-149722+5.78732T \quad (13)$$

where $G^{\Theta}_{AlB_2}$ and $G^{\Theta}_{AlB_{12}}$ are the molar Gibbs free energies of pure AlB_2 and AlB_{12}; $G^{\Theta Liq}_{Al}$ and $G^{\Theta Liq}_{B}$ are the molar Gibbs free energies of pure Al and B in the liquid state, respectively; $G^{\Theta S}_{Al}$ and $G^{\Theta S}_{B}$ are the molar Gibbs free energies of pure Al and B in solid state, respectively. The functions $G^{\Theta Liq}_{Al}$, $G^{\Theta Liq}_{B}$, $G^{\Theta S}_{Al}$ and $G^{\Theta S}_{B}$ can be obtained from Ref. [26].

The free energy changes of reactions (6) and (7) for the formation of 1 mol AlB_2 and 1 mol AlB_{12} versus the boron content in aluminum melt at 800 °C are shown in Fig. 7. It can be seen that, when the mole fraction of boron in aluminum melt reaches about 0.015, free energy would decrease when AlB_2 or AlB_{12} forms in the liquid metal. With the increase of boron content, the free energy change for the formation of 1 mol AlB_{12} increases faster than that for the formation of 1 mol AlB_2. This means that the thermodynamic driving force for the formation of AlB_{12} is larger than that for the formation of AlB_2.

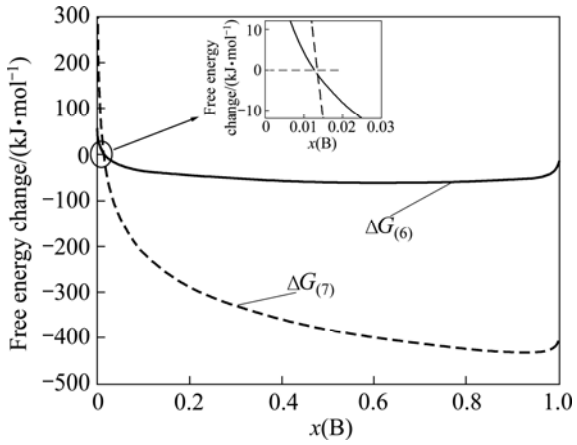

Fig. 7 Free energy changes of reactions (6) and (7) for formation of 1 mol AlB_2 and 1 mol AlB_{12} versus boron content in aluminum melt at 800 °C

The precipitation of the boride particles is also related to the interfacial energy between borides and molten aluminum. The solid−liquid interfacial energy can be expressed as [27]

$$\sigma = \sigma_{com} + \sigma_{str} \tag{14}$$

where σ_{com} and σ_{str} are the compositional contribution and the structural contribution to the interfacial energy, respectively. σ_{com} is given by

$$\sigma_{com} = (n_S + n_L)\Delta G / N_A \tag{15}$$

$$n_S = (N_A / V_S)^{2/3} \tag{16}$$

$$n_L = (N_A / V_L)^{2/3} \tag{17}$$

where n_S and n_L are the number of solid interface atoms and the number of liquid interface atoms per unit area, respectively; N_A is Avogadro's number; V_S is the average molar volume of atoms in solid; V_L is the average molar volume of atoms in liquid; ΔG is the free energy difference between the equilibrium molar free energy and the molar free energy when the atoms are forced to exist as a liquid of the same average composition, which can be calculated using the thermodynamic data by MIRKOVIC et al [24].

The structural contribution to the interfacial energy is given by

$$\sigma_{str} = \frac{kT_B}{bV_S^{2/3}} \tag{18}$$

where b is the number of atoms in one molecular of the solid; k is an empirical constant, which is taken as 6.5×10^{-4} according to Ref. [27]; T_B is the melting point of solid, which is taken as 1928 K for AlB_2 and 2573 K for AlB_{12} [28].

Calculations by above equations show that the interfacial energy between AlB_2 and molten aluminum is 0.775 and that between AlB_{12} and molten aluminum is 0.946. The interfacial energy has a strong influence on the precipitation course [29,30]. The smaller interfacial energy between AlB_2 and molten aluminum leads to the precipitation of AlB_2 particles at a lower boron content in the melt, although the free energy change facilitates the precipitation of the AlB_{12} particles. The AlB_{12} particles can only precipitate when the boron concentration reaches a higher level.

The reactions between KBF_4 and molten aluminum taking place at the droplet−aluminum interface proceed quickly before a layer of boride particles is formed [11]. The overall reaction rate is controlled by the transfer of BF_3 and KBF_4 in the bulk salt droplet to the interface. AlB_2 particles precipitate first at the droplet−aluminum interface with the increase of boron content. Compared with the immersion method, the average size of the salt droplets achieved by the vortex method is much smaller. For the vortex method, the vigorous stirring carried out during the mixing may cause a separation of the precipitated AlB_2 particles from the droplet−aluminum interface and promoting the transfer of boron atoms at the interface into the bulk aluminum melt. Also, for the small salt droplets achieved by the vortex method, the BF_3 and KBF_4 concentrations drop rapidly during the reactions and the transfer rates of BF_3 and KBF_4 in the bulk salt droplet to the interface decrease quickly. These lead to a rapid reduction of the amount of the boron atoms diffused into the aluminum melt. The boron content at the droplet-aluminum interface would not reach a value high enough for the precipitation of AlB_{12} particles. Because of the relatively low growth rate of AlB_2 particles in the melt of a relatively low boron content as well as the separation of AlB_2 particles from the interface due to the vigorous stirring, the formation of the agglomeration of AlB_2 particles can be prohibited.

Whereas, in the immersion method, no vigorous stirring was carried out during the immersion and the BF_3 and KBF_4 concentrations in the bigger salt droplets would drop slower during the reactions. This causes a higher boron content at the droplet-aluminum interface and thus the precipitation of AlB_{12} particles. The faster growth of the boride particles in the melt of a higher boron content also causes the formation of agglomerations.

5 Conclusions

1) Relatively high recovery rate of B can be obtained by mixing KBF_4 salt into molten aluminum due to the effect of prohibiting the BF_3 gas emission. For the immersion method, the recovery rate of B will decrease if vigorous stirring is carried out after each immersion.

2) The microstructure of the Al−B master alloys manufactured by the immersion method was characterized by the presence of AlB_{12} phase and agglomerations of boride particles. The mechanical stirring carried out after each immersion has an effect of breaking up the large agglomerations but could not prevent the formation of AlB_{12} phase. The master alloy produced by the vortex method exhibits a microstructure characterized by the absence of AlB_{12} phase and a well dispersion of AlB_2 particles. The differences in the stirring speed during the salt additions and the average size of the salt droplets achieved after the salt additions for the two mixing techniques cause the formation of the distinct microstructural features.

References

[1] SETZER W C, BOONE G W. The use of aluminum/boron master alloys to improve electrical conductivity [J], Light Metals, 1992: 337−343.

[2] COOPER P S, KEARNS M A. Removal of transition metal impurities in aluminum melts by boron additives [J]. Materials Science Forum, 1996, 217−222: 141−146.

[3] KARABAY S, UZMAN I. A study on the possible usage of continuously cast aluminum 99.6% containing high Ti, V and Cr impurities as feedstock for the manufacturing of electrical conductors [J]. Materials and Manufacturing Processes, 2005, 20: 231−243.

[4] DEPPISCH C, LIU G, SHANG J K, ECONOMY J. Processing and mechanical properties of AlB_2 flake reinforced Al-alloy composites [J]. Materials Science and Engineering A, 1997, 225: 153−161.

[5] AURADI V, KORI S A. Influence of reaction temperature for the manufacturing of Al−3Ti and Al−3B master alloys [J]. Journal of Alloys and Compounds, 2008, 453: 147−156.

[6] WANG Fang, WANG Ming-xing, LI Yun-liang, LIU Zhi-yong, LIU Zhong-xia, SONG Tian-fu. Grain refining mechanism of Al−B master alloy on Al alloys [J]. The Chinese Journal of Nonferrous Metals, 2008, 18(6): 974−979. (in Chinese)

[7] NAFISI S, GHOMASHCHI R. Boron-based refiners: Implications in conventional casting of Al−Si alloys [J]. Materials Science and Engineering A, 2007, 452−453: 445−453.

[8] WANG Chun-lei, WANG Ming-xing, LIU Zhi-yong, LIU Zhong-xia, WENG Yong-gang, SONG Tian-fu, YANG Sheng. The grain refining action of fine TiB_2 particles in the electrolytic low-titanium aluminum with Al−4B addition [J]. Materials Science and Engineering A, 2006, 427: 148−153.

[9] WANG Ming-xing, PANG Jin-hui, LIU Zhi-yong, LIU Zhong-xia, SONG Tian-fu, YANG Sheng. Grain refining action of Ti existing in electrolytic low-titanium aluminum with Al−4B addition for superheated Al melt [J]. Transactions of Nonferrous Metals Society of China, 2010, 20(6): 950−957.

[10] WANG Xiao-ming. The formation of AlB_2 in an Al−B master alloy [J]. Journal of Alloys and Compounds, 2005, 403: 283−287.

[11] El-MAHALLAWY N, TAHA M A, JARFORS A E W, FREDRIKSSON H. On the reaction between aluminum, K_2TiF_6 and KBF_4 [J]. Journal of Alloys and Compounds, 1999, 292: 221−229.

[12] GAO Ze-sheng. Production of high boron Al−B master alloys [J]. Light Alloy Fabrication Technology, 1994, 22(6): 14−17. (in Chinese)

[13] JACKSON M J, GRAHAM I D. Mechanical stirring of Al−B alloys [J]. Journal of Materials Science Letters, 1994, 13: 754−756.

[14] DEPPISCH C, LIU G, HALL A. The crystallization and growth of AlB_2 single crystal flakes in aluminum [J]. Journal of Materials Research, 1998, 13(12): 3485−3498.

[15] ZHU Hao, WANG Shu-mao, LI Zhi-nian, LIU Xiao-peng, JIANG Li-jun. Effects of sintering temperature and holding time on synthesis of AlB_2 [J]. Chinese Journal of Rare Metals, 2010, 34(5): 653−657. (in Chinese)

[16] HALL A C, ECONOMY J. Preparing high- and low-aspect ratio AlB_2 flakes from borax or boron oxide [J]. Journal of Metal, 2000: 42−44.

[17] KAYIKCI R, KURTULUS O, GURBUZ R. The formation and growth behavior of aluminium boride crystals in an Al−B alloy [J]. Solid State Phenomena, 2009, 144: 140−144.

[18] HONG Yong-xian. Al−B master alloys [J]. Light Alloy Fabrication Technology, 1985, 13(12): 19−26. (in Chinese)

[19] BIROL Y. Production of Al−B alloy by heating Al/KBF_4 powder blends [J]. Journal of Alloys and Compound, 2009, 481: 195−198.

[20] ALY I H, OMRAN A M, SHAHEEN M A, BASTAWEESY A. Production of Al−B master alloys from boron-bearing salts using different techniques [J]. Light Metals, 2004: 837−841.

[21] QIU Z X, YU Y X, ZHANG M J, GROTHEM S K, KVANDE H. Formation of aluminum−titanium alloys by electrolysis and by thermal reduction of titanium in cryolite-alumina melts [J]. Aluminium, 1988, 64: 606−609.

[22] BROOKS G A, RHAMDHANI M A, COLEY K S, SUBAGYO, PAN Y. Transient kinetics of slag metal reactions [J]. Metallurgical and Materials Transactions B, 2009, 40: 353−362.

[23] HASHIM J, LOONEY L, HASHMI M S J. Metal matrix composites: Production by the stir casting method [J]. Journal of Materials Processing Technology, 1999, 92−93: 1−7.

[24] MIRKOVIC D, GROBNER J, SCHMID-FETZER R, FABRICHNAYA O, LUKAS H L. Experimental study and thermodynamic re-assessment of the Al−B system [J]. Journal of Alloys and Compounds, 2004, 384: 168−174.

[25] LEE M S, TERRY B S, GRIEVESON P. Decomposition pressures of potassium and sodium fluoroborates and fluorotitanates [J]. Transactions of the Institution of Mining and Metallurgy C, 1994, 103: 26−32.

[26] DINSDALE A T. SGTE data for pure elements [J]. Calphad, 1991, 15: 317−425.

[27] WARREN R. Solid−liquid interfacial energies in binary and pseudo-binary systems [J]. Journal of Materials Science, 1980, 15: 2489−2496.
[28] AYLWARD G H. Chemical data book [M]. Australasia: Wiley, 1966: 1.
[29] ZHAO Jiu-zhou, WANG Qing-liang, LI Hai-li, HE Jie. Modeling of the precipitation kinetics during aging a predeformed Fe−Cu alloy [J]. Metallurgical and Materials Transactions A, 2011, 42: 3200−3207.
[30] WANG Qing-liang, ZHAO Jiu-zhou. A model describing the microstructure evolution in Fe−Cu alloys during thermal aging [J]. Materials Science and Engineering A, 2010, 528: 268−272.

铝熔体中混入 KBF_4 制备铝硼中间合金

王青亮[1]，赵洪生[2]，栗争光[2]，沈 利[2]，赵九洲[1]

1. 中国科学院 金属研究所，沈阳 110016；
2. 包头铝业集团有限公司 质量技术中心，包头 014046

摘 要：为了克服采用直接将 KBF_4 加到铝熔体表面的方法制备铝硼中间合金时存在的不足，分别采用两种混合技术——压入加盐法和漩涡加盐法制备 Al−3%B 中间合金。结果表明，采用压入加盐法所制备的合金中存在 AlB_{12}，硼化物在铝基体中主要以团簇形式存在，而采用漩涡加盐法所制备的合金中只有 AlB_2 颗粒形成，且 AlB_2 颗粒在铝基体中弥散分布。采用不同混合技术时，加盐过程中搅拌速度及加盐后所得氟盐液滴平均尺寸的差异导致了不同合金组织的形成。

关键词：铝硼中间合金；团簇；AlB_{12}；混合技术

(Edited by Xiang-qun LI)